NeuroImage 189 (2019) 432–444

Contents lists available at ScienceDirect

NeuroImage

journal homepage: www.elsevier.com/locate/neuroimage

Patterns of functional connectivity in an aging population: The Rotterdam Study

Hazel I. Zonneveld [a,b], Raimon HR. Pruim [a,c], Daniel Bos [a,b,e], Henri A. Vrooman [a,c], Ryan L. Muetzel [b,d], Albert Hofman [e], Serge ARB. Rombouts [f], Aad van der Lugt [a], Wiro J. Niessen [a,c,g], M. Arfan Ikram [a,b,h], Meike W. Vernooij [a,b,*]

[a] Department of Radiology and Nuclear Medicine, Erasmus MC University Medical Centre Rotterdam, the Netherlands
[b] Department of Epidemiology, Erasmus MC University Medical Centre Rotterdam, the Netherlands
[c] Department of Medical Informatics, Erasmus MC University Medical Centre Rotterdam, the Netherlands
[d] Department of Child and Adolescent Psychiatry/Psychology, Erasmus MC - Sophia, Rotterdam, the Netherlands
[e] Department of Epidemiology, Harvard T.H. Chan School of Public Health, Boston, MA, USA
[f] Department of Radiology, Leiden University Medical Center, Leiden, the Netherlands
[g] Imaging Physics, Faculty of Applied Sciences, Delft University of Technology, the Netherlands
[h] Department of Neurology, Erasmus MC University Medical Centre Rotterdam, the Netherlands

ARTICLE INFO

Keywords:
Aging
Brain networks
Epidemiology
Functional connectivity
Population-based
Resting-state functional MRI

ABSTRACT

Structural brain markers are studied extensively in the field of neurodegeneration, but are thought to occur rather late in the process. Functional measures such as functional connectivity are gaining interest as potentially more subtle markers of neurodegeneration. However, brain structure and function are also affected by 'normal' brain ageing. More information is needed on how functional connectivity relates to aging, particularly in the absence of overt neurodegenerative disease. We investigated the association of age with resting-state functional connectivity in 2878 non-demented persons between 50 and 95 years of age (54.1% women) from the population-based Rotterdam Study. We obtained nine well-known resting state networks using data-driven methodology. Within the anterior default mode network, ventral attention network, and sensorimotor network, functional connectivity was significantly lower with older age. In contrast, functional connectivity was higher with older age within the visual network. Between resting state networks, we found patterns of both increases and decreases in connectivity in approximate equal proportions. Our results reinforce the notion that the aging brain undergoes a reorganization process, and serves as a solid basis for exploring functional connectivity as a preclinical marker of neurodegenerative disease.

1. Introduction

Normal aging is associated with brain changes that can be linked to neurodegeneration (Peters, 2006). Non-invasive imaging techniques (e.g., MRI) have enabled us to study structural brain changes such as grey matter atrophy and white matter lesions in relation to aging and dementia (Brant-Zawadzki et al., 1985). More recently, it has been hypothesized that these anatomical brain changes are preceded by changes in the brain's functional organization (Jack et al., 2010). Developed over three decades ago, functional MRI (fMRI) is a non-invasive method for investigating the functional dynamics of the brain. fMRI indirectly reflects neural activity by measuring MRI signal fluctuations induced by changes in blood oxygenation and flow resulting from changes in neural metabolic demand (Logothetis, 2002). In the absence of an explicit stimulus, resting-state fMRI quantifies the synchronization of spontaneous signal fluctuations over time, or functional connectivity, across multiple brain regions (Fox and Raichle, 2007).

Measures of functional connectivity have been shown to differ between patients with Alzheimer's disease and controls (Dennis and Thompson, 2014; Wang et al., 2007). In parallel, many studies of aging have shown reduced functional connectivity *within* resting-state networks such as the default mode network (DMN), the salience network, and the motor network (Betzel et al., 2014; Chan et al., 2014; Ferreira et al., 2016; Geerligs et al., 2015; Grady et al., 2016). In contrast,

* Corresponding author. Erasmus MC, University Medical Center, Room Na28-18, P.O. box 2040, 3000 CA, Rotterdam, the Netherlands.
E-mail address: m.vernooij@erasmusmc.nl (M.W. Vernooij).

https://doi.org/10.1016/j.neuroimage.2019.01.041
Received 30 September 2018; Received in revised form 9 January 2019; Accepted 15 January 2019
Available online 16 January 2019

functional connectivity *between* networks has been found to increase with age, which may reflect decreased segregation (Andrews-Hanna et al., 2007; Chan et al., 2014; Ferreira and Busatto, 2013; Ng et al., 2016). These age-related decreases in within-network connectivity and increases in between-network connectivity have also been demonstrated to be related to, for example, cognitive performance and motor ability (Andrews-Hanna et al., 2007; Chan et al., 2014; Ferreira and Busatto, 2013; Geerligs et al., 2015; Keller et al., 2015; Wu et al., 2007). Importantly, previous studies on functional connectivity in normal aging were conducted with relatively small samples, or included wide age ranges rather than middle-aged and elderly persons who are at greatest risk for neurodegeneration. Also, the lack of a population-based design in most studies may hamper the generalizability of the findings (Chan et al., 2014; Ferreira et al., 2016; Grady et al., 2016; Sala-Llonch et al., 2015; Siman-Tov et al., 2016). Moreover, brain function depends on the segregation and integration of brain networks. Limiting analyses to an individual resting-state network, such as the DMN, may be inadequate in gaining a more comprehensive understanding of the functional organization of the aging brain (Baldassarre A, 2015; Greicius et al., 2004; Hafkemeijer et al., 2012; Koch et al., 2010; Ng et al., 2016; Tsvetanov et al., 2016). Finally, previous studies defined networks based on anatomical parcellations that do not necessarily conform to the true functional architecture of the human brain (Song et al., 2014; Wang et al., 2010).

Additional knowledge about the aging brain in the healthy elderly may increase our insight into the neural basis of neurodegenerative diseases. Based on the current literature, we hypothesized that older age in the general population is negatively associated with within-network connectivity, and positively associated with between-network connectivity. Given previous literature, we more specifically hypothesized that in middle-aged and elderly persons from the general population, networks showing greatest decreases in functional connectivity would most likely be those that have been previously implicated in aging or neurodegeneration in smaller (clinical) studies, i.e. the DMN, salience network and motor network. Yet, to allow for changes in other networks to be detected, as well as to avoid a bias towards network decreases, we deployed an exploratory approach, analyzing large-scale networks in the entire brain as well as allowing for both decreases and increases in connectivity. In addition, we explored how various factors such as sex, cardiovascular risk, and apolipoprotein E ε4 carrier status associate with functional connectivity in an aging population.

2. Materials and methods

2.1. Study population

This study was conducted within the Rotterdam Study, a prospective population-based cohort study aimed at investigating determinants and consequences of age-related diseases in the elderly (Ikram et al., 2017). The cohort originated in 1990 and was comprised of 7983 participants 55 years of age and older. In 2000 and 2006 the cohort was expanded and now consists of 14,926 participants 45 years of age and older. Resting-state functional MRI (rs-fMRI) was piloted in 2010–2011, and fully implemented into the study protocol from 2012 onwards (Ikram et al., 2015). Between 2010 and 2016, a total of 3288 participants underwent rs-fMRI. We excluded participants with poor data quality (e.g. poor registration based on visual inspections, excessive head motion or high levels of ghosting; n = 293), with cortical infarcts on MRI (n = 80), and with prevalent dementia or insufficient dementia screening (n = 37). In total, 2878 participants were included for the current analysis.

Data can be obtained upon request. Requests should be directed towards the management team of the Rotterdam Study (secretariat.epi@erasmusmc.nl), which has a protocol for approving data requests. Because of restrictions based on privacy regulations and informed consent of the participants, data cannot be made freely available in a public repository. The Rotterdam Study has been approved by the Medical Ethics Committee of the Erasmus MC (registration number MEC 02.1015) and by the Dutch Ministry of Health, Welfare and Sport (Population Screening Act WBO, license number 1071272-159521-PG). The Rotterdam Study has been entered into the Netherlands National Trial Register (NTR; www.trialregister.nl) and into the WHO International Clinical Trials Registry Platform (ICTRP; www.who.int/ictrp/network/primary/en/) under shared catalogue number NTR6831. All participants provided written informed consent to participate in the study and to have their information obtained from treating physicians.

2.2. MRI acquisition, tissue segmentation and infarct rating

Neuroimaging was performed on a 1.5-Tesla MRI scanner (Signa Excite II, GE Healthcare, Milwaukee, WI, USA) using an eight-channel head coil. Structural imaging included a T1-weighted 3D fast RF spoiled gradient recalled acquisition in steady state with an inversion recovery pre-pulse (FSPGR-IR) sequence (repetition time (TR) = 13.8 ms, echo time (TE) = 2.8 ms, inversion time (TI) = 400 ms, field-of-view (FOV) = 25 cm^2, matrix = 416 × 256 (interpolated to 512 × 512), flip angle = 20°, number of excitations (NEX) = 1, bandwidth (BW) = 12.50 kHz, 96 slices with slice thickness 1.6 mm zero-padded in the frequency domain to 0.8 mm), a proton density (PD) weighted sequence (TR = 12,300 ms, TE = 17.3 ms, FOV = 25 cm^2, matrix = 416 × 256, NEX = 1, BW = 17.86 kHz, 90 slices with slice thickness 1.6 mm), and a T2-weighted fluid-attenuated inversion recovery (FLAIR) sequence (TR = 8000 ms, TE = 120 ms, TI = 2000 ms, FOV = 25 cm^2, matrix = 320 × 224, NEX = 1, BW = 31.25 kHz, 64 slices with slice thickness 2.5 mm). rs-fMRI data were obtained using an echo-planar imaging sequence (TR = 2900 ms, TE = 60 ms, FOV = 21 cm^2, 31 axial slices, flip angle = 90°, matrix size = 64 × 64, slice thickness = 3.3 mm, 165 vol). Acquisition time was 7:44 min. Participants were instructed to lie still with their eyes open and to stay awake.

2.3. Structural MRI quantification

T1-weighted MRI scans were processed using FreeSurfer (v5.1) (Fischl et al., 2004) to obtain brain tissue segmentations and volumetric summaries of intracranial and supratentorial grey matter volume. Presence of infarcts was visually assessed on structural MRI sequences, and those involving cortical gray matter were classified as cortical infarcts (Ikram et al., 2015).

2.4. rs-fMRI data preprocessing

Preprocessing was carried out using the FMRIB Software Library (FSL; http://www.fmrib.ox.ac.uk/fsl) (Jenkinson et al., 2012) and involved: removal of the first five volumes to allow for signal equilibration, head movement correction by volume-alignment using FSL's MCFLIRT (Jenkinson et al., 2002), global 4D mean intensity normalization, spatial smoothing (Gaussian kernel with 6 mm full-width at half-maximum) and temporal high-pass filtering (>0.01Hz). To quantify head motion in the rs-fMRI data we used the maximum absolute as well as the mean relative (i.e. frame-wise) head displacement as calculated by MCFLIRT. After preprocessing, functional images were co-registered to the corresponding T1-weighted images using FSL's FLIRT (Jenkinson et al., 2002; Jenkinson and Smith, 2001) and subsequently registered to 2 mm isotropic MNI-152 standard space by applying the transformation obtained from non-linear registration of the T1-weighted images to MNI-152 template using FSL's FNIRT (Andersson et al., 2010). All registrations were visually inspected in order to exclude scans with registration failures or with large artefacts. Scans that showed absolute head displacement greater than 3 mm and/or mean frame-wise displacement greater than 0.2 mm were excluded. A technical issue caused participants to be scanned with the phase and frequency encoding directions swapped during the resting state fMRI acquisition. This rotated acquisition scheme led to a mild ghost artifact in the phase encoding direction. Ghost-to-signal ratio

(G/S-ratio) was defined as follows: first the fMRI image was divided into 4 regions: 1) background, 2) ghost outside the brain, 3) ghost + signal within the brain, 4) signal within brain. G/S-ratio was then calculated by dividing the median intensity within region 2 by the median intensity within region 4. G/S-ratio was treated as a covariate in the analyses (see statistical analyses section). Moreover, scans with G/S-ratio>0.1 were excluded.

In addition to the standard rs-fMRI pre-processing, FMRIB's ICA-based Xnoiseifier (FIX v1.06) was used to remove structured noise from the data. First, we applied independent component analysis (ICA) to the preprocessed single-subject data, using automatic dimensionality estimation, as implemented in FSL's MELODIC (v5.0.5). Next, FIX was used to automatically detect the components representing noise, which were then removed from the data (with the option for soft cleanup and additional removal of motion confounds) (Griffanti et al., 2014; Salimi-Khorshidi et al., 2014). To optimize its classification performance we trained FIX using a study-specific training dataset of 60 randomly selected subjects (equally distributed across age-binned 5 year strata, and among women and men). Two raters independently hand-labeled the components derived from these scans as 'signal', 'unknown' or 'noise', by visual inspection of each components' spatial map, time-course and power spectrum (Griffanti et al., 2017). Inconsistently labeled components were further discussed/inspected to achieve a final consensus labeling. This training dataset was used to train FIX and to evaluate its performance by means of a leave-one-out cross validation. We found the training set to perform well, with a mean proportion of correctly labeled 'signal' and 'noise' components of respectively 94% and 76%.

2.5. Connectivity analysis

For our functional connectivity analysis, we first generated a study-specific functional parcellation using high-dimensionality ICA (Kiviniemi et al., 2009; Smith et al., 2013). To generate this parcellation, we employed a temporally concatenated group-ICA using FSL's MELODIC on a selection of 500 datasets with maximal brain coverage, matching the total sample on age and sex distribution, to guarantee optimal brain coverage of the atlas. The dimensionality of the ICA was set to 100 components, similar to the population-based UK Biobank (Miller et al., 2016). These 100 components were hand-labeled as either 'signal', 'noise', or 'unknown' using the same rating procedure as discussed above for the subject-level denoising. Out of 100 components, 50 components were labeled as 'signal', which we will further refer to as 'functional nodes'.

We exploited these spatial templates in a multivariate linear regression against each subjects' rs-fMRI data (e.g. first stage of the dual regression framework (Beckmann et al., 2009; Filippini et al., 2009) to derive subject-level time-series of the 100 components. For every subject, we then obtained a 50×50 connectivity matrix by calculating the full temporal correlation, converted to Z-scores using Fisher Z-transformation, between every pair of signal time-series using the tools implemented in FSLNets (http://fsl.fmrib.ox.ac.uk/fsl/fslwiki/FSLNets). For a more comprehensive analysis and to aid comparison across studies, we mainly focused on analyses on a network-level. We therefore clustered the 50 functional nodes into large-scale networks by hierarchically clustering the full group-level correlation matrix (Smith et al., 2013). Subsequently, we derived network-level subject-specific connectivity matrices by calculating the mean correlation value of the respective node-pairs within and between every (pair of) network(s). Furthermore, we computed the standard deviation of each node's time series as a measure of nodal strength (i.e., signal amplitude), as implemented in FSLNets. Finally, for every network we averaged its associated nodal strengths to define a measure of network-strength, which we refer to as mean signal amplitude.

2.6. Other measurements

A number of cardiovascular risk factors, based on information derived from home interviews and physical examinations during visits to our research center, were assessed. Body mass index was calculated by dividing weight (in kilograms) by height (in meters) squared. Systolic and diastolic blood pressure (in mmHg) were measured twice on the right arm with a random-zero sphygmomanometer, and the two readings were averaged for analyses. Serum glucose (mmol/L), total cholesterol (mmol/L), and HDL-cholesterol (mmol/L) levels were measured using standard laboratory techniques (Ikram et al., 2017). Diabetes mellitus was defined as a fasting serum glucose level $\geq$7.0 mmol/L, or use of anti-diabetic medication. Smoking habits were assessed by interview and categorized as current smoker, former smoker, and never smoked. Information on use of antihypertensive medication and lipid-lowering medication was obtained by interview. *APOE* genotype was determined by polymerase chain reaction on coded DNA samples in the original cohort, and by bi-allelic Tacqman assays (rs7412 and rs429358) for the expansion cohorts. In 93 participants *APOE* genotype was determined by genetic imputation (Illumina 610K and 660K chip; imputation with Haplotype Reference Consortium (HRC) reference panel (v1.0) with Minimac 3). *APOE*-ε4 carrier status was defined as carrier of one or two ε4 alleles.

2.7. Statistical analyses

Missing values on cardiovascular risk factors (maximum 4.0%) were imputed using 5-fold multiple imputation, based on age, sex, and the other available cardiovascular risk factors. Distribution of covariates was similar in the imputed versus the non-imputed dataset.

Group-level non-parametric permutation testing (n = 10,000 unique permutations), as implemented in FSL's randomise (Winkler et al., 2014) was used to associate sex and age with functional connectivity within and between networks. We applied two levels of correction for multiple testing. First, we corrected for multiple testing (family-wise error (FWE), n = 9 within network and n = 36 between network analyses) using randomise. Secondly, an alpha of pFWE <0.0125 was considered statistically significant by Bonferroni correcting FWE-adjusted p-values for the two main effects (age and sex) and two-tailed tests. We first investigated the association between age and functional connectivity. Therefore, we started investigating whether age was positively or negatively correlated with functional connectivity, within and between networks. Subsequently, we classified age-related associations with functional connectivity as follows: 1) increasing magnitude of positive network correlation, 2) decreasing magnitude of positive network correlation, 3) increasing magnitude of nodal/network anti-correlation, 4) decreasing magnitude of network anti-correlation 5) shift in networks from anti-correlation to positive correlation and 6) shift from positive correlation to anti-correlation. We next investigated whether there were sex-related differences in functional connectivity, within and between resting state networks. To assess the focal nature of the network associations, we investigated the association of age and sex with functional connectivity at the node-level. After examining the correlation amongst nodes/networks, we investigated the association of age and sex with mean signal amplitude within each network. For each analysis, in order to investigate whether the association between age and functional connectivity was modified by sex, we tested the statistical interaction by adding an age*sex interaction term to the regression models. All analyses described above were performed using three models. In the first model, we adjusted for age or sex, mean frame-wise head displacement, and ghost-to-signal ratio. In the second model, we additionally adjusted for supratentorial grey matter volume and intracranial volume to investigate whether the associations with functional connectivity were independent of macrostructural brain makers. In the third model, we additionally adjusted for the cardiovascular risk factors (i.e., body mass index, systolic and diastolic blood pressure, total and high-density lipoprotein cholesterol, diabetes mellitus, smoking, antihypertensive and lipid-lowering medication) and apolipoprotein E-ε4 carrier status, to study whether there were pathways relating age to functional connectivity measures, other than those involving these factors, and to remove any confounding effects

by these factors. To further explore the effect of cardiovascular risk factors and APOE on functional connectivity, all analyses were run with both connectivity measures, adjusted for age, sex, mean frame-wise head displacement, ghost-to-signal ratio, supratentorial grey matter volume and intracranial volume. With respect to smoking status, for these analyses smoking was classified as current versus ever/former smoking. Hypertension was defined as a systolic blood pressure>140 mmHg, diastolic blood pressure>90 mmHg, or use of blood pressure lowering medication. To allow for comparison across continuous cardiovascular risk factors (body mass index, systolic and diastolic blood pressure, cholesterol levels), we calculated z scores (subtracting the population mean and dividing by the standard deviation). Additionally, to reproduce our findings we split the whole sample into two randomly selected groups by using SPSS and repeated the analysis with age. Finally, we stratified by age (dichotomized at 65 years of age), and we repeated age analyses for both strata adjusted for age, sex, mean frame-wise head displacement and ghost-to-signal ratio (Model I). Furthermore, to account for a possible non-linear age-effect, age*age was added to the linear regression models and all analyses were repeated. To put effect estimates of our age-related associations with functional connectivity in a context, we compared effect estimates of age on functional connectivity (Model I) with the effect estimates of age on supratentorial grey matter volume, since grey matter volume is an established imaging marker of which its association with age has been extensively described before. To aid comparison, we calculated Z-scores of age, supratentorial grey matter volume and correlation values. In addition, we adjusted supratentorial grey matter volume for intracranial volume.

Analyses were done using IBM SPSS Statistics version 21.0 (IBM Corp, Armonk, NY), and FSL's randomise. Kernel density plots and heat maps were created using R v3.2.2 (R Foundation for Statistical Computing, Vienna, Austria).

3. Results

3.1. Study characteristics and network definitions

Characteristics of the study population are presented in Table 1. Out of 2878 participants, 54.1% were women and the mean age was 66.9 years (ranging from 50.5 to 95.2 years).

For resting-state fMRI analyses, we first clustered the 50 functional nodes into 9 large-scale networks using hierarchical clustering of the full group-level correlation matrix (Supplementary Figure 1): the anterior default mode network (DMNa), posterior default mode network (DMNp), frontoparietal network (FPN), dorsal attention network (DAN), ventral attention network (VAN), sensorimotor network (SMN), visual network (Vis), subcortical network (Subcort), and temporal network (Temp) (Fig. 1). Using this clustering, we obtained the subject-specific network-level connectivity matrices (see Methods) and Fig. 2 displays the average network-level matrix across all individuals.

3.2. Age with network connectivity

The heat maps in Fig. 3 show the association between age and functional connectivity on a nodal-level for all the three models. The numbers along the x- and y-axis represent node-numbers presented in Fig. 1. In Fig. 3, for example, clusters of negative association are seen mainly involving nodes in the DMNa and SMN network, which remain after additional model adjustments. Between networks, robust clusters of positive associations are seen for the DAN-DMN nodes and Vis-Temp nodes. A mixture of positive and negative associations within a network are observed between SMN-DMN nodes. As described in section *2.4 connectivity analysis*, we mainly focused on the association between age and functional connectivity on a network-level. Fig. 4 and Supplementary Figure 2 illustrate the age association on functional connectivity using kernel density plots, within and between all pairs of networks. The kernel density plots show whether (1) a network is positively or negatively correlated (as depicted by the horizontal line at correlation value 0 (y-axis)), and (2) whether there is a positive or negative association with age (direction of the regression-line). In addition, the heat map in Fig. 5 shows the associations of age with functional connectivity within and between all pairs of networks for the three models, separated into positively and negatively connected network-pairs. Supplementary Table 1 shows the parameter estimates including 95% confidence intervals for Model I. Within networks, as displayed on the diagonal of Fig. 5, we observed that older age was associated with an increased magnitude of positive correlation values for the visual network (difference in $Z_{(r)}$ per year increase in age, 0.002; 95% confidence interval [CI]: 0.001; 0.002; $P_{FWE\text{-}corrected} < 0.0125$). Furthermore, we found that older age was associated with a decreased magnitude of positive correlation values for: DMNa (−0.004, 95% CI: -0.005;-0.003; $P_{FWE\text{-}corrected} < 0.001$), VAN (−0.003, 95% CI: -0.004;-0.003; $P_{FWE\text{-}corrected} < 0.001$), and SMN (−0.003, 95% CI: -0.003;-0.002; $P_{FWE\text{-}corrected} < 0.0125$). Associations remained largely the same after additionally adjusting for grey matter volume and intracranial volume, cardiovascular risk factors and *APOE-ε4* carrier status.

Between networks, older age was associated with increased magnitude of positive correlation values between the DMNa-FPN, DMNp-DAN, DMNp-Vis, FPN-VAN, and Subcort-Temp networks, all $P_{FWE\text{-}corrected} < 0.0125$. Furthermore, older age was related to decreased magnitude of a positive correlation values between the DMNp-DMNa, DAN-VAN, and VAN-SMN, all $P_{FWE\text{-}corrected} < 0.0125$. Age was also negatively correlated with between network connectivity where the following network pairs were more strongly anti-correlated in older individuals: DMNa-Vis, DAN-Subcort, VAN-Vis, VAN-Temp, and SMN-Temp, all $P_{FWE\text{-}corrected} < 0.0125$. An association of older age with decreased magnitude of anti-correlation values was found for the: DMNa-DAN, DMNa-VAN, DMNp-Subcort, FPN-SMN, and SMN-Subcort (all $P_{FWE\text{-}corrected} < 0.0125$). Lastly, we observed an age-related shift from positive network connectivity to negative network connectivity for the DMNa-Temp, and FPN-Temp networks. Conversely, a shift from negative to positive connectivity was found between the Vis-Temp networks. After adjustments for structural brain markers, cardiovascular risk factors and *APOE-ε4* status, associations became slightly weaker, but in essence unchanged.

Table 1
Characteristics of the study population.

Characteristics	N = 2878
Age, years	66.9 (9.3)
Female sex	1558 (54.1)
Body mass index, kg/m^2	27.2 (3.9)
Systolic blood pressure, mmHg	138.9 (20.2)
Diastolic blood pressure, mmHg	82.6 (10.8)
Total cholesterol, mmol/L	5.5 (1.1)
High-density lipoprotein, mmol/L	1.5 (0.4)
Diabetes mellitus	356 (12.4)
Smoking	
Never	928 (32.9)
Former	1430 (50.8)
Current	459 (16.3)
Antihypertensive medication	1129 (39.9)
Lipid-lowering medication	803 (28.4)
Hypertension	1859 (64.6)
APOE-ε4 carrier	748 (27.8)
Intracranial volume, mL	1478 (118)
Supratentorial grey matter volume, mL	594 (38)

Values are depicted as mean (SD) for continuous variables, and absolute numbers (%) for categorical variables. N = sample size; APOE = apolipoprotein E; SD = standard deviation. The following variables had missing data: body mass index (n = 83), blood pressure (n = 87), serum total cholesterol (n = 115), serum high-density lipoprotein (HDL) cholesterol (n = 115), diabetes mellitus (n = 14), smoking (n = 61), antihypertensive and lipid-lowering medication (n = 50), and APOE-ε4 carrier (n = 192).

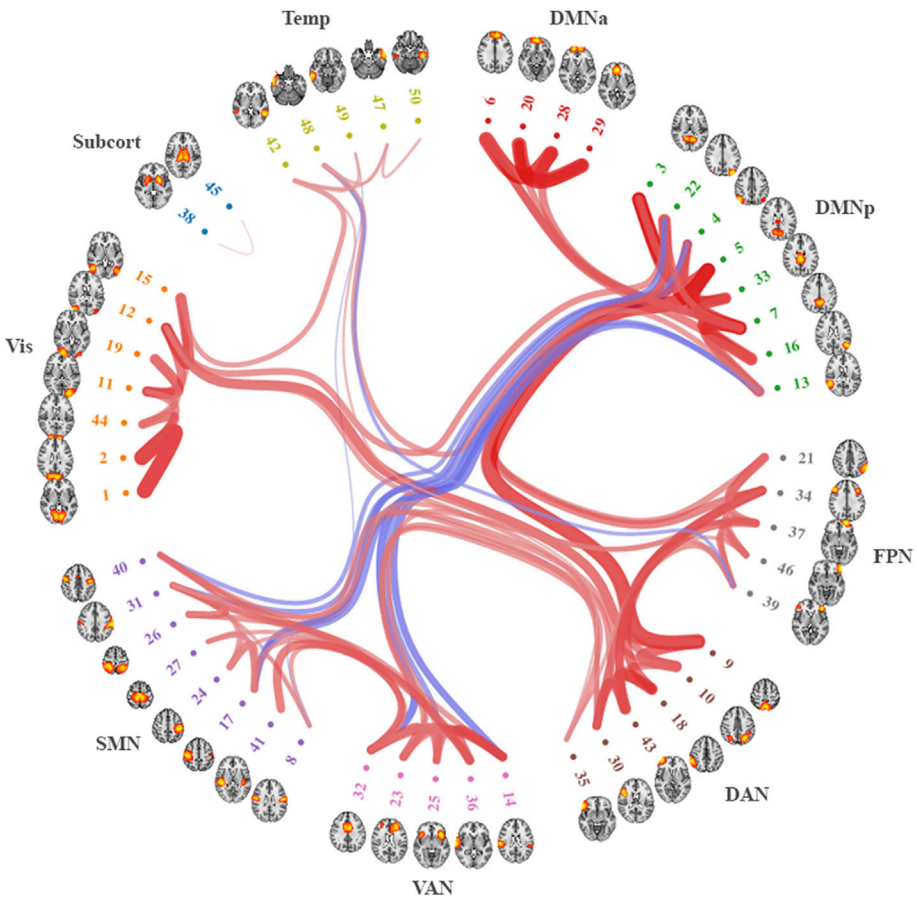

Fig. 1. Functional connectome of the human brain. Functional connectome of the human brain and associated spatial maps (axial views). The 50 functional nodes are clustered into nine networks, based on a T-test (mean group effect) on the edges between all nodes (i.e., the correlation matrix) across all 2 878 individuals, as implemented in FSLNets (http://fsl.fmrib.ox.ac.uk/fsl/fslwiki/FSLNets) (edges presented by T-values thresholded at 2/3 of the full range, with positive correlations in red, and anti-correlations in blue). Abbreviations: DMNa default mode network anterior; DMNp default mode network posterior; FPN frontoparietal network; DAN dorsal attention network; VAN ventral attention network; SMN sensorimotor network; Vis visual network; Subcort subcortical network; Temp temporal network.

3.3. Sex differences in network connectivity

We found that, compared to women, men had stronger within-network positive connectivity in the FPN, DAN and SMN networks. Between networks, differences between men and women were predominantly observed involving the DAN, VAN, and Subcort (Supplementary Figure 3). When examining the association of sex with correlation values on a node-level, we observed similar findings as on a network-level (Supplementary Figure 4). Finally, although we observed significant differences in correlation values between men and women, the statistical interaction by age and sex was limited to DMNa-SMN (Models I and II), and DMNp-Subcort (Models II and III). For these networks, we observed that middle-aged women had higher anti-correlation values compared to middle-aged men, whereas at older age women had lower anti-correlations values compared to men (data not shown).

3.4. Mean signal amplitude

Older age was associated with lower mean signal amplitude in all networks, with the exception of subcortical and temporal network. After adjusting for cardiovascular risk factors and *APOE-ε4* status, associations in the DMNp, FPN, and Vis networks were no longer statistically significant (Supplementary Table 2). Additionally, men had a higher mean signal amplitude compared to women within the DMNa, FPN, DAN, VAN, and SMN networks for all models (Supplementary Table 3).

3.5. Functional connectivity and risk factors for neurodegenerative disease

Fig. 6 shows the association between cardiovascular risk factors, APOE and functional connectivity on a network-level. Higher body mass index (BMI) was associated with lower within VAN connectivity. Hypertension was associated with lower within SMN connectivity. Higher high-density lipoprotein was found to be associated with higher within VAN connectivity. Between networks, most significant findings were found for BMI (e.g., decreased magnitude of correlation values between the DMNa-DMNP and DAN-Vis networks, and increased anti-correlation values between the SMN-FPN, SMN-DAN, DMNp-Subcort, Vis-Subcort, and Vis-Temp networks, all $P_{FWE\text{-}corrected}<0.0125$). Diabetes mellitus was associated with decreased positive correlation values of DMNa-DMNp and DMNp-Temp. No significant findings were found for serum total cholesterol, APOE-ε4 carriership, and current smoking. Supplementary Table 4 shows the association between the various cardiovascular risk factors, APOE, and mean signal amplitude. Higher BMI and blood pressure were associated with lower mean signal amplitude in several networks.

3.6. Reproducibility of the findings, age stratification and comparison of effect estimates

Supplementary Table 5 shows the characteristics of the two split samples. With regards to the characteristics there were no significant differences between the two groups. Fig. 7 illustrates that both split samples show similar results to the whole sample and to each other, albeit with lower statistical power.

Supplementary Figure 5 shows the age-stratified results. Age-effects seemed to be stronger in the older sample (above 65 years of age) versus the younger participants, though the direction and pattern of associations was similar in both groups. Furthermore, the exploration of a possible non-linear relationship of age with functional connectivity on a network-level showed that a significant association of age*age with functional connectivity was limited to within-network functional connectivity of SMN (Supplementary Figure 6).

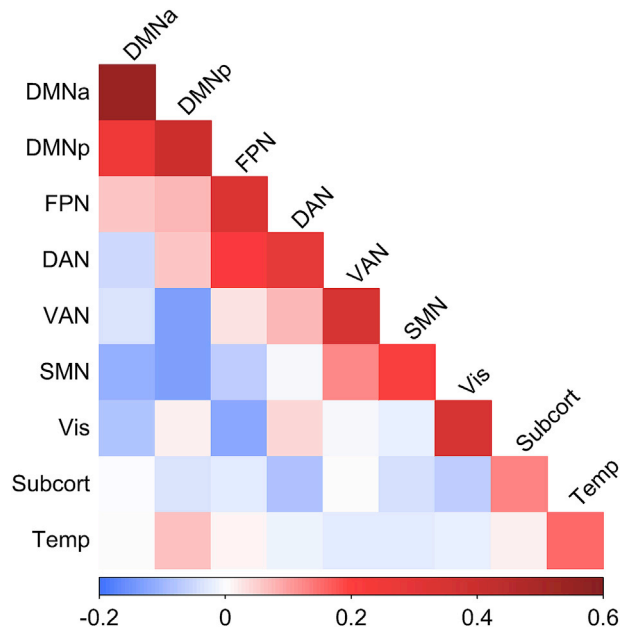

Fig. 2. Mean correlation value of the node-pairs respectively within and between every (pair of) network(s), averaged across all individuals. Colors and sizes of the blocks correspond to mean correlation (Z(*r*)) values of the node-pairs (nodes are specified in Fig. 1, indicated by numbers) respectively within (on the diagonal) and between every (pair of) network(s), with blue and red indicating negative and positive correlations, respectively. Abbreviations: DMNa default mode network anterior; DMNp default mode network posterior; FPN frontoparietal network; DAN dorsal attention network; VAN ventral attention network; SMN sensorimotor network; Vis visual network; Subcort subcortical network; Temp temporal network.

We found the strongest effect estimate of age for DMNa within-network connectivity with a mean difference in z score per standard deviation increase in age: -0.21 (standard deviation (sd) 0.02), and VAN within-network connectivity: $\beta_{age} = -0.23$ (sd 0.02). The weakest effect estimates for within-network connectivity were found for FPN ($\beta_{age} = -0.01$ (sd 0.02)), and Temp ($\beta_{age} = -0.01$ (sd 0.02)). Between networks, the strongest effect estimates were observed for DMNa-DMNp: $\beta_{age} = -0.20$ (sd 0.02), and Vis-Temp ($\beta_{age} = 0.20$ (sd 0.02)). The weakest effect estimate was found for DMNp-SMN ($\beta_{age} = -0.01$ (sd 0.02)). The effect estimate of age in relation to supratentorial grey matter volume was $\beta_{age\ (per\ standard\ deviation\ increase\ in\ age)} = -0.27$ (sd 0.01).

4. Discussion

In this large population-based study, we studied patterns of functional brain connectivity at the network level in an aging population using resting-state fMRI. We found that within the anterior default mode network, ventral attention network, and sensorimotor network, functional connectivity decreased with increasing age, and that this was most pronounced after the age of 65 years. Conversely, within the visual network, functional connectivity increased with older age. Between networks, we found patterns of both increases and decreases of (anti-) correlations in approximate equal proportions. Furthermore, we found that men showed higher within-network functional connectivity in the frontoparietal, dorsal attention and sensorimotor networks compared to women. Between networks, men and women differed predominantly in the attentional networks and the subcortical network. The strongest effect size for age with within-network connectivity (observed for the default mode network) had a similar magnitude of effect as the relation between age and supratentorial grey matter volume. It is well-known that age is the major risk factor for dementia and that synaptic dysfunction represents an early sign of this disease associated with hallmark neuropathological findings. Therefore, it can be hypothesized that changes in functional connectivity in brain aging found in the current study may represent one part of the spectrum from aging to clinical dementia. Thus, this study adds to our understanding of functional connectivity of the aging brain in middle-aged and elderly individuals, and can serve as the basis for studies examining functional connectivity as a potential early marker of neurodegenerative disease.

Although several studies have shown links between resting state functional connectivity and cognition or dementia, fewer studies have addressed functional connectivity within an aging population free of stroke and dementia (Ferreira et al., 2016; Geerligs et al., 2015; Grady et al., 2016; Sala-Llonch et al., 2015). Most studies that have investigated the effect of age on functional connectivity measured differences within or between brain networks using hypothesis-driven region of interest based correlations, data-driven techniques such as independent component analysis or by using graph theory. To incorporate our current results

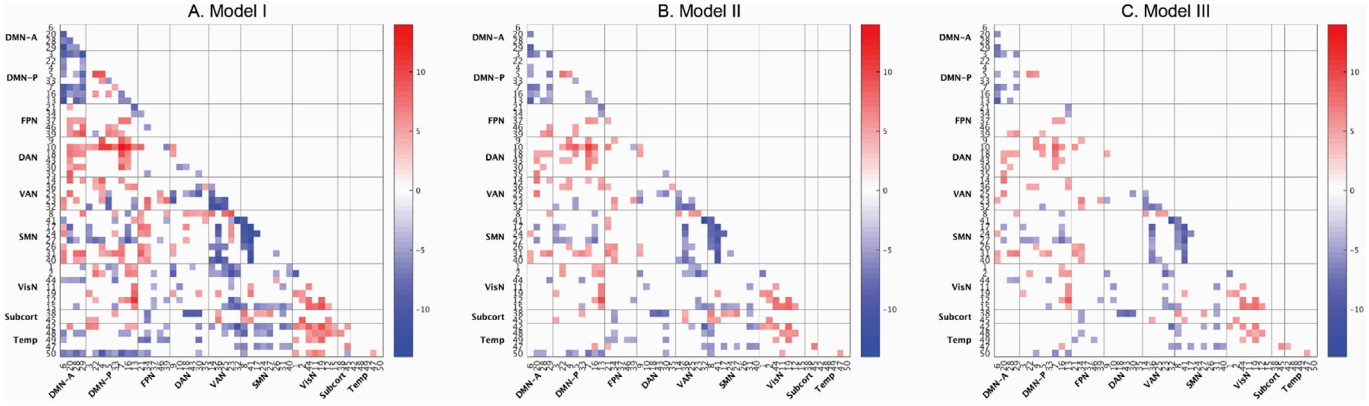

Fig. 3. Association between age and functional connectivity on a node-level. Colors and sizes of the blocks correspond to *t*-values from the linear regression models of age in relation to functional connectivity, with blue and red indicating negative and positive associations, respectively. Darker colored blocks indicate stronger associations, and all colored blocks survived multiple testing ($P_{-FWEcorrected} < 0.0125$). Numbers along x- and y-axis represent node-numbers presented in Fig. 1. Panel A. Model I: adjusted for sex, mean frame-wise head displacement, and ghost-to-signal ratio. Panel B. Model II: as Model I, additionally adjusted for supratentorial grey matter volume and intracranial volume. Panel C. Model III: as Model II, additionally adjusted for body mass index, systolic and diastolic blood pressure, total and high-density lipoprotein cholesterol, diabetes mellitus, smoking, antihypertensive and lipid-lowering medication and apolipoprotein E-ε4 carriership. Abbreviations: DMN-A default mode network anterior; DMN-P default mode network posterior; FPN frontoparietal network; DAN dorsal attention network; VAN ventral attention network; SMN sensorimotor network; VisN visual network; Subcort subcortical network; Temp temporal network.

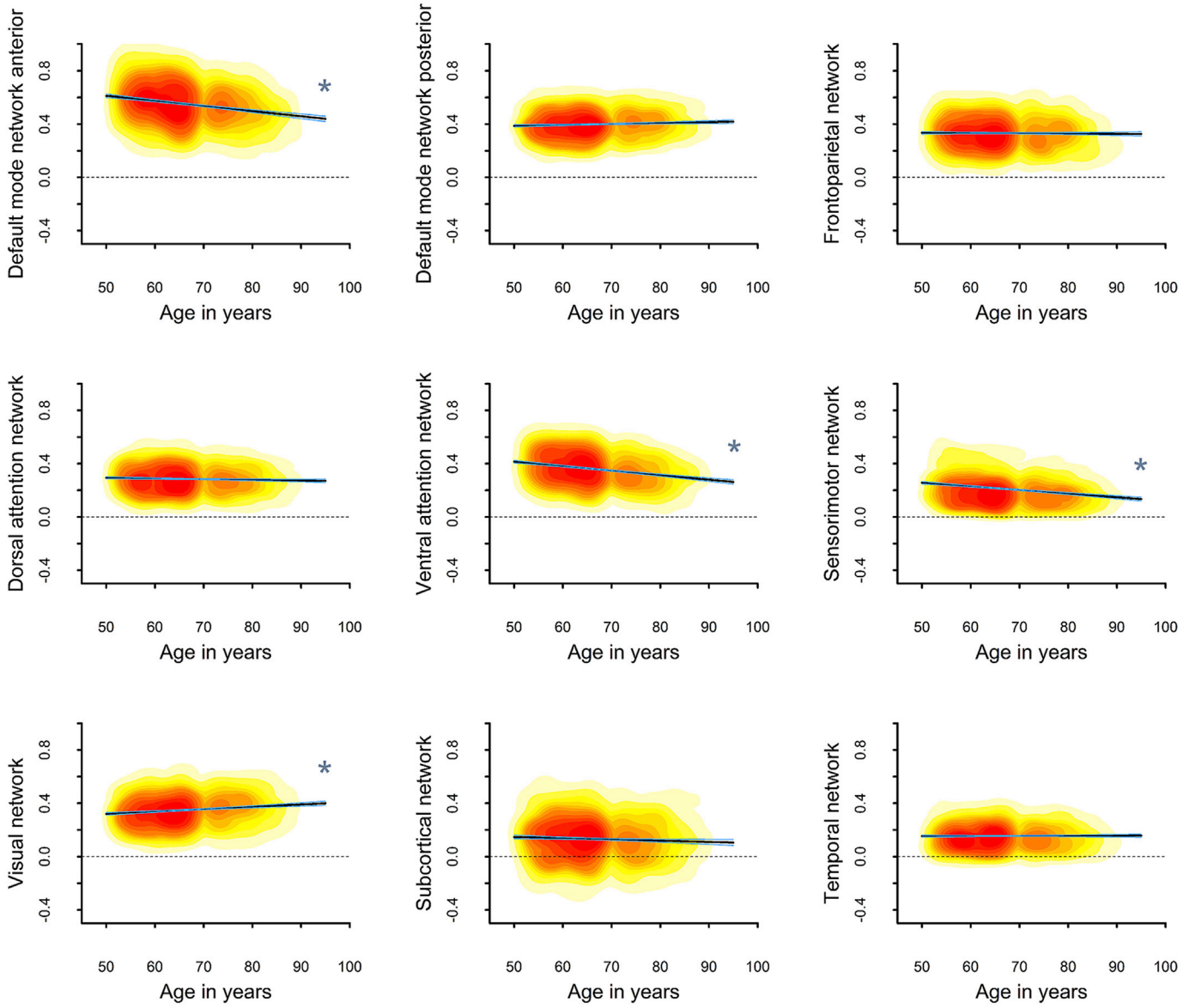

Fig. 4. Age associations with correlation values of functional connectivity within networks. Kernel density plots visualize the distribution of the data (red = dense) and the direction of the age effect on the connectivity values; black line denotes the linear regression line (with blue 95% confidence interval), adjusted for mean frame-wise head displacement, ghost-to-signal ratio and sex, across nine networks. Dotted horizontal line indicates a connectivity value of zero as reference. Significant associations are indicated by asterisks (*).

into the heterogeneous findings from previous studies, some points deserve discussion. First, previous studies assessed age-related changes in functional connectivity from childhood into old age, or by comparing a group of younger individuals to a group of much older individuals; this is distinct from the approach utilized by the current study in which all participants were between 50 and 95 years of age, and age was modeled continuously. When comparing a group of young participants with a group of older participants, it might be difficult to disentangle neurodevelopment and neurodegeneration when investigating the effect of aging on functional connectivity. This is supported by our finding that the effect of age on connectivity was less strong in younger versus older participants in our sample. In addition, it is hypothesized that aging affects cerebrovascular dynamics (e.g., atherosclerosis or reduced vascular reactivity) (Ferreira et al., 2016). Therefore, results from functional connectivity studies that compared (very) young and older subjects should be interpreted in the light of these limitations. Because our study sample exists of middle-aged and elderly participants, we therefore think that this issue is less of a concern. Second, the methodology to investigate functional connectivity differs considerably across studies, particularly with respect to how nodes/networks are defined and how nodal/network time-series are extracted from the data. Nodes can be defined using either an anatomical (e.g., MNI-coordinates, AAL atlas (Tzourio-Mazoyer et al., 2002)) or a functional atlas (e.g., (Yeo et al., 2011), and either as 'hard' (non-overlapping sets of voxels; e.g., AAL atlas (Tzourio-Mazoyer et al., 2002) or 'soft' (overlapping weighted spatial maps; e.g., ICA-based atlases (Kiviniemi et al., 2009; Smith et al., 2013)) parcels. Nodal time-series can be obtained using either a univariate seed-based approach (i.e., mean time-series) or multivariate regression. Given the notion that anatomically defined brain areas do not always align with function, and that our study population ranged in age between 50 and 95 years deviates from previously research, we obtained a study-specific functional brain atlas. Importantly, this data-driven approach yielded resting-state networks which highly correspond to the networks known from literature (Yeo et al., 2011).

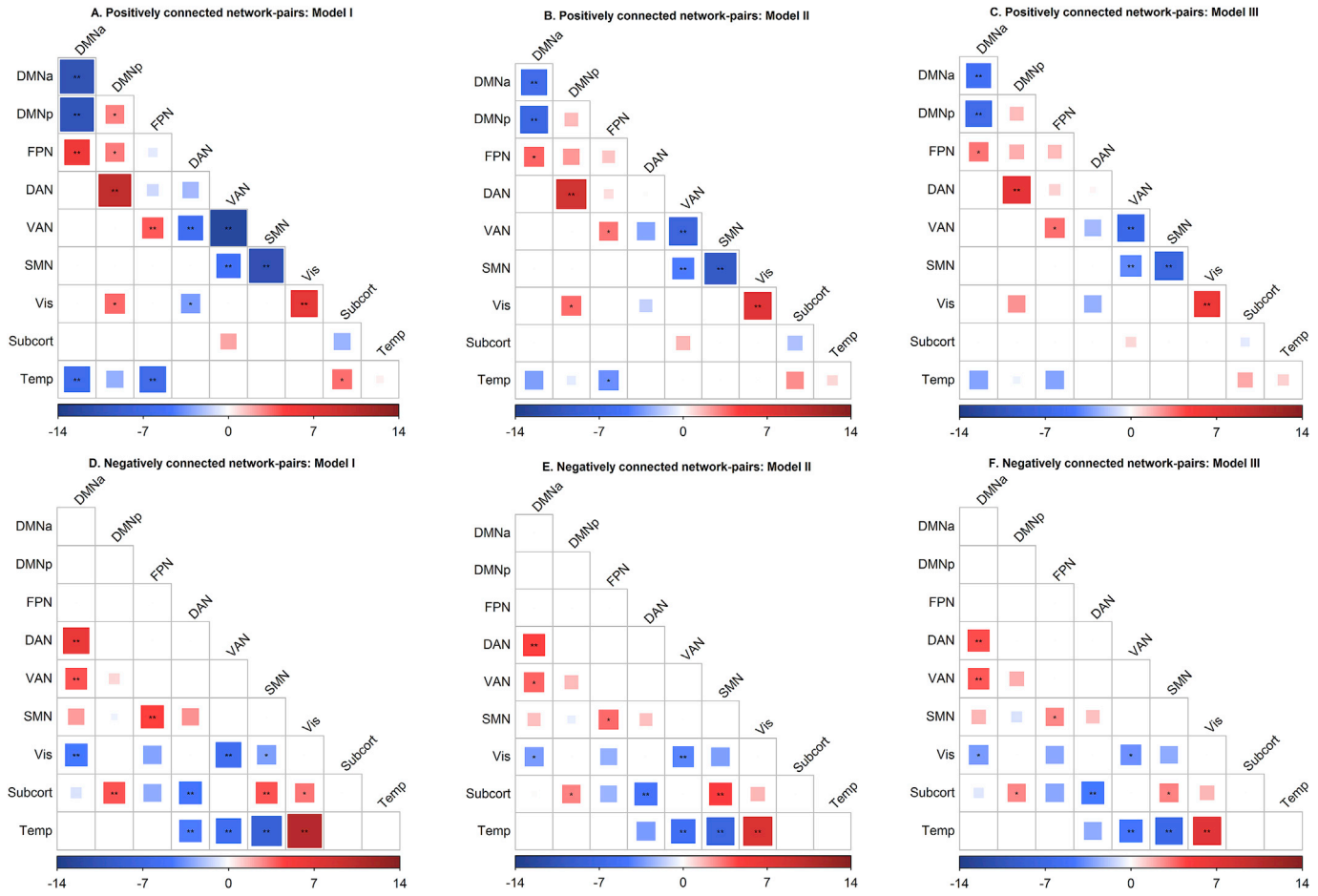

Fig. 5. Association between age and functional connectivity on a network-level, separated into positively and negatively connected network-pairs. Colors and sizes of the blocks correspond to *t*-values from the linear regression models of age in relation to functional connectivity, with blue and red indicating negative and positive associations, respectively. Larger blocks indicate stronger associations, and significance levels as indicated by asterisks: *$P_{-FWEcorrected}<0.0125$ **$P_{-FWEcorrected}<0.0025$. Panel A/D. Model I: adjusted for sex, mean frame-wise head displacement, and ghost-to-signal ratio. Panel B/E. Model II: as Model I, additionally adjusted for supratentorial grey matter volume and intracranial volume. Panel C/F. Model III: as Model II, additionally adjusted for body mass index, systolic and diastolic blood pressure, total and high-density lipoprotein cholesterol, diabetes mellitus, smoking, antihypertensive and lipid-lowering medication and apolipoprotein E-ε4 status. Abbreviations: DMNa default mode network anterior; DMNp default mode network posterior; FPN frontoparietal network; DAN dorsal attention network; VAN ventral attention network; SMN sensorimotor network; Vis visual network; Subcort subcortical network; Temp temporal network.

Given the above-mentioned considerations, our results can be placed in the context of existing literature in the following way. We observed that DMNa, VAN and SMN within-network connectivity showed significant negative associations with older age, which has been reported previously in aging populations but also in Alzheimer's disease (Chan et al., 2014; Ferreira et al., 2016; Grady et al., 2016). Conversely, the visual network within-network connectivity showed significant positive association with older age. With respect to between-network connectivity, we found both age-related increases and decreases in functional connectivity, as well as both positive and negative correlations between networks. Notably, this can result in complex findings regarding the directionality of associations, challenging their interpretation (e.g., a positive inter-network age effect could indicate two networks becoming less negatively or more positively correlated). Interestingly, generally in literature an increased functional connectivity between networks in elderly has been reported (Chan et al., 2014; Geerligs et al., 2015; Song et al., 2014). It is hypothesized these changes together reflect a decreasing segregation of brain networks. Importantly, this decreasing segregation has previously primarily been investigated over wide age ranges, spanning from young adulthood to very old age (Chan et al., 2014). A general explanation is that with aging, the brain changes its functional specialization. Our study importantly adds to this by showing that this segregation is still subject to change in middle and old age, showing similar patterns as those observed over the full lifespan. Given previous findings that decreases in segregation relate to cognitive decline (Chan et al., 2014), our study findings implicate that this is also relevant up to high age, may potentially be modified (given our results with cardiovascular risk factors), and may link aging and neurodegeneration.

A post-hoc analysis showed that age-related effects on functional connectivity on a nodal-level, while adjusting for sex, ghost-to-signal ratio and motion, were negatively associated with the nodal distance ($r = -0.18$, $p < 0.001$). In other words, we observed stronger age-related decreases in long-range connections such as between the nodes of DMNa-DMNp and DAN-VAN networks. Our observation that in particular longer distance networks were affected by decrease in functional connectivity could relate to these connections potentially being more vulnerable to damaging pathology such as amyloid deposition, reduced white matter integrity or white matter lesions (Chan et al., 2017; Tomasi and Volkow, 2012). In this respect, the fact that amyloid pathology has been described to occur as one of the earliest regions in the DMN, is of particular interest (Mormino et al., 2011; Sheline et al., 2010b; Sperling, 2011). Whereas previous studies on aging changes in the DMN were inconclusive, our study more convincingly supports the DMNa to decrease in connectivity in aging, as well as its connections with other networks, lending further

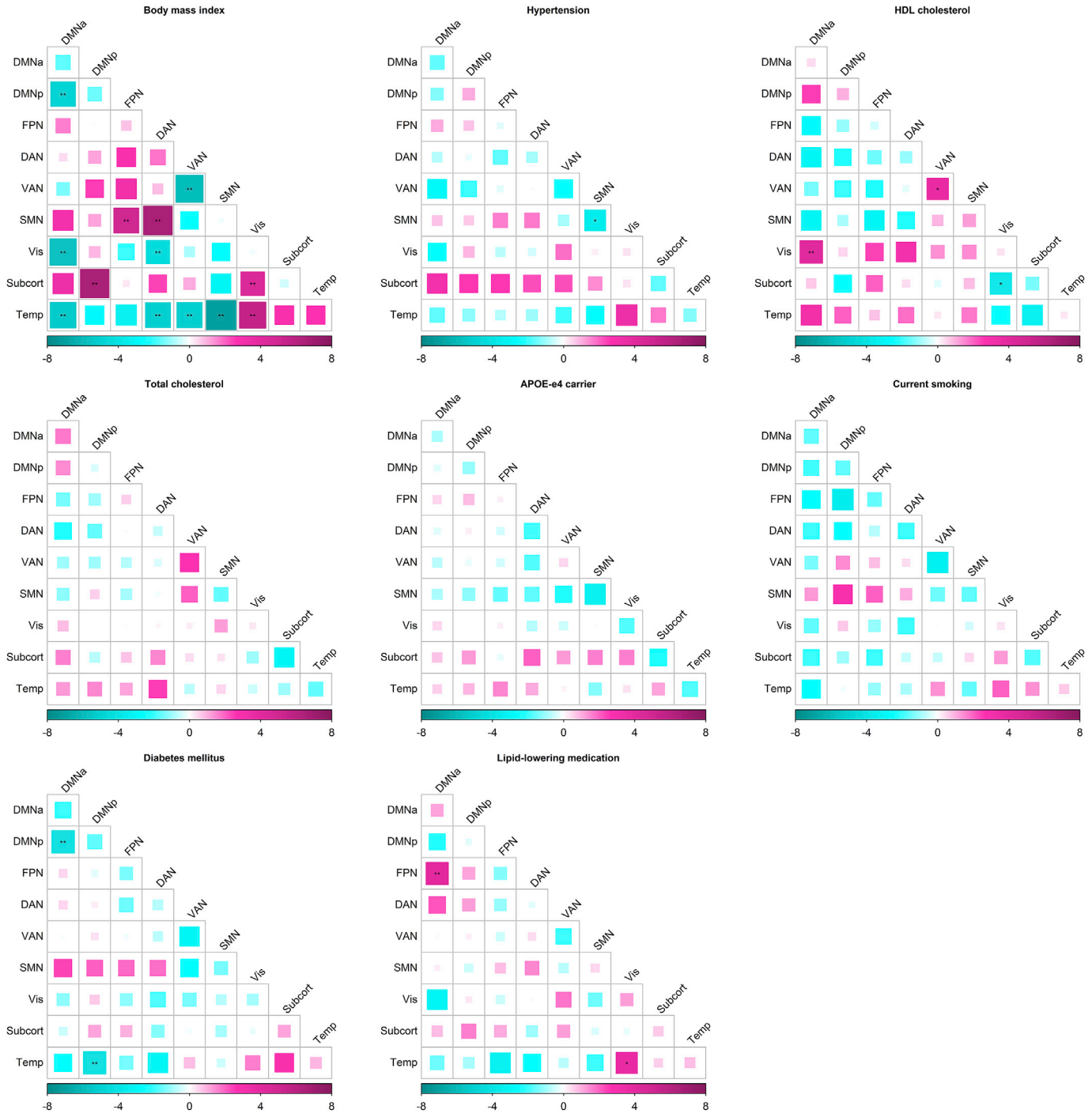

Fig. 6. Association of cardiovascular risk factors and APOE-ε4 status with functional connectivity on a network-level. Colors and sizes of the blocks correspond to *t*-values from the linear regression models of cardiovascular risk factors and APOE-ε4 status in relation to functional connectivity, with turquoise and fuchsia indicating negative and positive associations, respectively. Larger blocks indicate stronger associations, and significance levels as indicated by asterisks: *$P_{-FWEcorrected}<0.0125$ **$P_{-FWEcorrected}<0.0025$. Model is adjusted for age, sex, mean frame-wise head displacement, ghost-to-signal ratio, supratentorial grey matter volume and intracranial volume. Abbreviations: 95% CI 95% confidence interval; DMNa default mode network anterior; DMNp default mode network posterior; FPN frontoparietal network; DAN dorsal attention network; VAN ventral attention network; SMN sensorimotor network; Vis visual network; Subcort subcortical network; Temp temporal network; APOE-ε4 apolipoprotein E-ε4.

support to the hypothesis that this may an important site of accumulation of pathology, even in asymptomatic subjects. In parallel, we found age-related increases in functional connectivity in short-range connections such as between the nodes of the DMNa-FPN and the DMNp-DAN. This may suggest that at older age functional connectivity primarily increases between networks that are anatomically close, whereas it decreases between networks that are further apart, although to our knowledge such findings have not been reported before.

Of the major resting state networks reported in the literature, the DMN is most frequently investigated. The DMN comprises a set of brain regions including the ventral/dorsal medial prefrontal cortex and the anterior cingulate cortex (together the DMNa), and the posterior cingulate cortex, precuneus and inferior parietal lobules (DMNp). The DMN is deactivated during (cognitive) tasks, shows high levels of activity at rest,

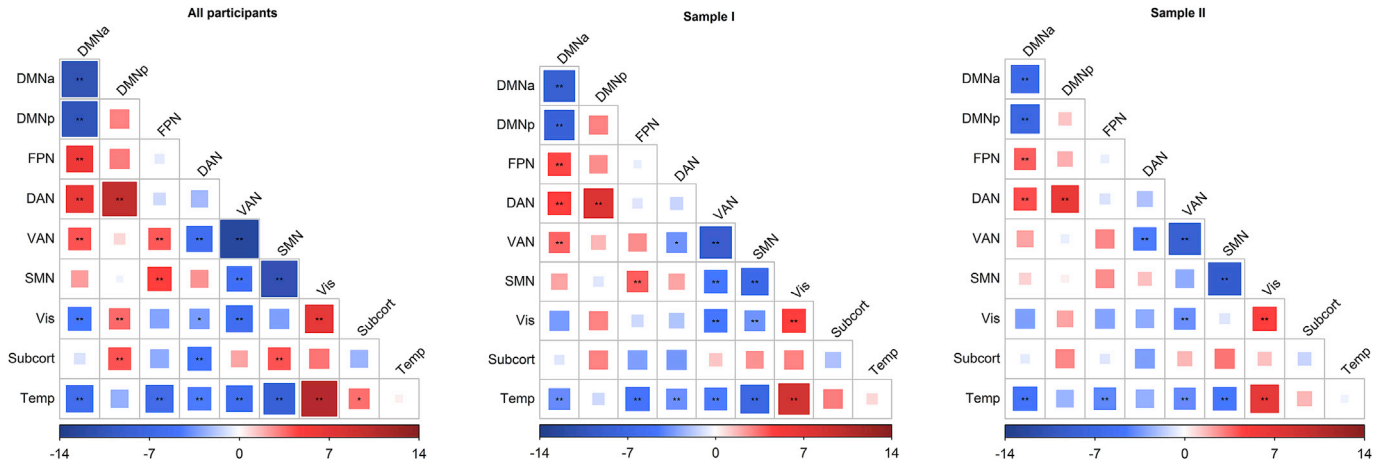

Fig. 7. Reproducibility of the association between age and functional connectivity on a network-level. Colors and sizes of the blocks correspond to *t*-values from the linear regression models of age in relation to functional connectivity, with blue and red indicating negative and positive associations, respectively. Larger blocks indicate stronger associations, and significance levels as indicated by asterisks: *$P_{-FWEcorrected}<0.0125$ **$P_{-FWEcorrected}<0.0025$. First panel reflects the whole sample and corresponds to Fig. 4 (Panel A), second and third panel reflect the randomly selected samples. Model adjusted for sex, mean frame-wise head displacement, ghost-to-signal ratio, supratentorial grey matter volume and intracranial volume. Abbreviations: DMNa default mode network anterior; DMNp default mode network posterior; FPN frontoparietal network; DAN dorsal attention network; VAN ventral attention network; SMN sensorimotor network; Vis visual network; Subcort subcortical network; Temp temporal network.

and has been studied extensively in relation to dementia (Greicius et al., 2004; Hafkemeijer et al., 2012). Several studies have also investigated age-related changes in DMN connectivity, but the results are inconclusive (Andrews-Hanna et al., 2007; Ferreira et al., 2016; Jockwitz et al., 2017; Klaassens et al., 2017). Within the DMNa, older age was associated with decreased magnitude of a positive correlation value whereas within the DMNp we did not observe any association with age. Interestingly, connectivity between DMNA-DMNp showed a negative association with older age, which is consistent with previous studies in healthy aging (Andrews-Hanna et al., 2007; Esposito et al., 2008; Ferreira et al., 2016). Such age-related decreases in functional connectivity within DMN could potentially influence the ability of the brain to shift from a task-negative to a task-positive state, thereby hampering cognitive performance (Andrews-Hanna et al., 2007). A population-based study of 711 older adults (55–85 years of age) found no age-related changes in the DMN (Jockwitz et al., 2017). Importantly, in that study, the DMN was not divided into its anterior and posterior subsystems, indicating the potential relevance of investigating DMN at different scales of functional organization.

When examining networks implicated in primary information processing, we found increased functional connectivity in the visual network. This is in contrast with a study that found decreased functional connectivity in the visual network when comparing a group of old and young adults (Nashiro et al., 2017). In line with previous research, the sensorimotor network showed decreased within-network functional connectivity (Nashiro et al., 2017). On a node-level, we observed primarily decreased correlation values between nodes from the auditory cortex and primary motor cortex. Within temporal and subcortical networks, no aging effects on functional connectivity measures were observed. However, these two networks showed age-associations with other networks.

Taken together, these findings suggest that with an increase in age, the brain seems to undergo a complex reorganization process with integration and segregation of resting-state networks (Sala-Llonch et al., 2015; Sun et al., 2012). Though it remains unclear whether changes in functional connectivity seen in aging can be explained by reductions in grey matter volume, associations in the present study did not substantially change after adjusting for global grey matter volume. It may thus be assumed that age-associations in resting-state connectivity found in the current study were not entirely driven by differences in atrophy rates (Friston, 2011; Jockwitz et al., 2017; Klaassens et al., 2017).

The BOLD signal is considered an indirect measure of neural activity, and depends on neurovascular coupling and cerebrovascular reactivity, both of which are known to undergo age-related changes (Liu, 2013). In line with this, we found that older age was associated with lower mean signal amplitude within several resting state networks. In addition, several cardiovascular risk factors were associated with the mean signal amplitude, and adjusting signal amplitude for cardiovascular risk factors led to weaker associations. This might suggest that cardiovascular risk factors affect neurovascular coupling, cerebrovascular reactivity, and subsequent BOLD signal (Liu, 2013). It has been suggested that there are regional, age-specific differences in vascular reactivity, which may only partly reflect those captured on a global level. Although we have attempted to control for differences on a global level, regional specificity might deviate from the overall global pattern (Tsvetanov et al., 2015).

Little is known about sex differences in functional connectivity. The observed pattern of differences in the functional connectome found in the current study is different compared to another large population-based study (Ritchie et al., 2017). We observed greater connectivity in men within the FPN, DAN and SMN, whereas higher connectivity within the DMN in women and higher connectivity within the SMN and visual network was previously reported. Comparing the between-network analysis from both studies is challenging due to the fact that the connectivity in that study was measured regardless of valence (Ritchie et al., 2017). Furthermore, the authors calculated the strength of a connection differently from the approach used in the current study.

With respect to the effect of cardiovascular risk factors and APOE-ε4 status on functional connectivity, we observed the strongest associations for body mass index with a wide range of networks. Furthermore, we observed in participants with diabetes mellitus lower functional connectivity between DMNa-DMNp. It has been hypothesized that type 2 diabetes mellitus and insulin resistance are associated with systemic hyperinsulinemia and reduced brain insulin levels, which are risk factors for dementia (Blazquez et al., 2014; Craft, 2007). A previous study found that type 2 diabetes mellitus patients showed lower correlation values between seeds of DMNa and DMNp compared to healthy controls (Musen et al., 2012), which is in line with our results. Although we did not observe a significant association with hypertension and functional connectivity of a network-level, we did observe that higher systolic blood pressure was associated with lower mean signal amplitude in several

networks, whilst higher BMI was associated with higher mean signal amplitude in several networks. This might indicate that although high BMI is associated with poor cardiovascular risk, BMI and high blood pressure associate differently with functional connectivity. Furthermore, in contrast to previous literature which showed that the APOE-ε4 allele modulates functional connectivity decades before clinical symptoms arise (Filippini et al., 2009; Sheline et al., 2010a), our present study did not find such a significant association with APOE-ε4 status. Notably, we observed lower within-network connectivity and lower mean signal amplitude in APOE-ε4 carriers, albeit non-significant. This may indicate that at the age of our study participants (45 years and above), the effect of APOE is already reduced. Yet, more research is needed to investigate the role of APOE-ε4 in the relationship between functional connectivity and cognition.

Though this study has several strengths, some limitations deserve to be acknowledged. First, it is known that motion can affect functional connectivity (Van Dijk et al., 2012). A post-hoc analysis showed that older age was associated with greater frame-wise head displacement ($r = 0.21$, $P < 0.001$). In rs-fMRI, handling motion-related effects is a complex issue for which as of yet no perfect correction method has been found (Caballero-Gaudes and Reynolds, 2017; Power et al., 2017). By applying FMRIB's ICA-based Xnoiseifier, adding a motion covariate in our group-level analyses, and excluding participants with extensive head motion we aimed to limit potential bias and to increase sensitivity, whilst also staying in line with methods applied in similar studies in order to facilitate comparison of results (Alfaro-Almagro et al., 2018; Miller et al., 2016). In addition, we performed several additional post-hoc analyses to ensure our results are not contingent upon using FIX-ICA and adding motion as covariate to the regression models only. For this we performed the following analyses:

(I) We compared 'high-movers' with 'low-movers' within age strata to investigate motion effect on functional connectivity independent of the age effect. This analysis revealed no significant motion-related effects on functional connectivity within the age strata (see Supplementary Figure 7 including description of the sample). (II) Second, we created a motion-matched sample in order to explore the age-effects on functional connectivity within a motion-matched study sample (n = 664 subjects from the original population, matched on severity of motion). Within this matched sample, we found similar age-effects on functional connectivity compared to the whole study population, indicating that our results are not driven by motion-effects (see Supplementary Figure 8 for the results and the description of the motion-matched sample). (III) Finally, we replicated the nodal distance plot in the motion-matched sample (Supplementary Figure 9). We observed a similar pattern in the motion-matched sample compared to the whole sample. This again shows that the age-effects found in the current study are, at least not importantly, dependent on motion effects.

Furthermore, in this field of much debate and controversy, global signal regression has recently been suggested to remove noise from data. Global signal regression removes the average fMRI signal across all the voxels in the brain, with an important recognized drawback that it may remove temporal signal, which comprises signal of interest and not just noise. This may even result in distance-dependent artifacts. Therefore, in the current study we preferred an ICA-based procedure, which allows for removing noise while specifically retaining signal of interest, although we acknowledge that there is at present no universally accepted optimal method for removing motion from the data. In addition, though there is no standard procedure that has been shown to fully remove the effect of head motion from the data (Pruim et al., 2015), an ongoing debate persists on whether such residual effects might reflect neurobiological correlates rather than noise (Couvy-Duchesne et al., 2014; Van Dijk et al., 2012). Second, a weak age-association with functional connectivity on a network-level may also be driven by a mixture of positive and negative age-associations on a nodal level, which may cancel out each other. Importantly, if any, this might lead to an underestimation rather than an overestimation of the age-effect. Third, it is still under debate whether negative correlations are artificial in origin. Also, there is much discussion on how these anti-correlations relate to the preprocessing (e.g., global signal regression). Since there is much debate about it, we chose to report the full picture rather than a selective one (e.g., only positive correlations), but are at the same time cautious about making inferences based on these negative correlations. Fourth, measuring correlation values between networks does not provide the crucial causal information about the dynamic nature of functional connectivity. Functional connectivity may exist between anatomically unconnected nodes, but can be driven by other pathways of the functional connectome (Adachi et al., 2012). To investigate this, studies that investigate partial correlation (direct vs indirect connections) and effective connectivity (causal connections) are needed (Friston, 2011). Fifth, the number of edges is dependent of the number of nodes within a certain network. In the current study, we clustered 50 functional nodes into networks. The identified networks differ in the number of nodes per network, e.g. the subcortical network consists of two nodes, whereas the sensorimotor network consists of eight nodes. This will affect the level of detail of our findings and potentially the accuracy of our results.

Sixth, imaging at 1.5T has a lower signal-to-noise ratio than higher field strengths. Due to the population-based nature of the study, in the current scan-protocol we had to carefully balance the restrictions of time, costs and inconvenience for the participants with the relevance and quality of the acquired imaging data. In addition, more noise in the time series may result in less reliable (and probably lower) connectivity values (Bijsterbosch et al., 2017). Thus, combined with the constraints on temporal and spatial resolution of our rs-fMRI sequence (due to the population-based nature of the study), this may have reduced our sensitivity to find biological effects (Wardlaw et al., 2012).

In conclusion, this exploratory population-based study allowed us to examine age-related patterns of functional brain connectivity. This work extends beyond previous work by showing that age is not only related to decreases in within-network functional connectivity, but also to diffuse increases and decreases in (anti-)correlations between different networks. Moreover, this study could provide useful information for studies of neurodegeneration to contrast their findings against. Our results provide additional support to the notion that the aging brain undergoes a complex functional reorganization process. Future longitudinal studies are needed to elucidate the mediation role of structural brain features as well as to explore the association between functional connectivity and cognition or dementia.

Disclosure statement

The Rotterdam Study is supported by the Erasmus MC and Erasmus University Rotterdam; the Netherlands Organization for Scientific Research (NWO); the Netherlands Organization for Health Research and Development (ZonMW); the Research Institute for Diseases in the Elderly (RIDE); the Ministry of Education, Culture and Science; the Ministry of Health, Welfare and Sports; the European Commission (DG XII); and the Municipality of Rotterdam. Dr. Meike W. Vernooij received a research fellowship from the Erasmus MC University Medical Center, Rotterdam, the Netherlands and a ZonMW clinical fellowship. This research was funded by a grant from Alzheimer Nederland (grant number WE.03-2012-30). Wiro Niessen is co-founder, chief scientific director, and shareholder of Quantib BV. Serge Rombouts is supported by a VICI grant from the Netherlands Organization for Scientific Research (NWO) (grant number 016-130-677). The authors report no financial interests or potential conflicts of interest in relation to this manuscript.

Acknowledgements

We are grateful to the study participants, the staff from the Rotterdam Study, and participating general practitioners and pharmacists.

Appendix A. Supplementary data

Supplementary data to this article can be found online at https://doi.org/10.1016/j.neuroimage.2019.01.041.

References

Adachi, Y., Osada, T., Sporns, O., Watanabe, T., Matsui, T., Miyamoto, K., Miyashita, Y., 2012. Functional connectivity between anatomically unconnected areas is shaped by collective network-level effects in the macaque cortex. Cerebr. Cortex 22, 1586–1592.

Alfaro-Almagro, F., Jenkinson, M., Bangerter, N.K., Andersson, J.L.R., Griffanti, L., Douaud, G., Sotiropoulos, S.N., Jbabdi, S., Hernandez-Fernandez, M., Vallee, E., Vidaurre, D., Webster, M., McCarthy, P., Rorden, C., Daducci, A., Alexander, D.C., Zhang, H., Dragonu, I., Matthews, P.M., Miller, K.L., Smith, S.M., 2018. Image processing and Quality Control for the first 10,000 brain imaging datasets from UK Biobank. Neuroimage 166, 400–424.

Andersson, J., Jenkinson, M., Smith, S., 2010. Non-linear registration, aka spatial normalisation. FMRIB technical report TR07JA2.

Andrews-Hanna, J.R., Snyder, A.Z., Vincent, J.L., Lustig, C., Head, D., Raichle, M.E., Buckner, R.L., 2007. Disruption of large-scale brain systems in advanced aging. Neuron 56, 924–935.

Baldassarre A, C.M., 2015. Resting state network changes in aging and cognitive decline. Hear. Bal. Commun. 13, 58–64.

Beckmann, C.F., Mackay, C.E., Filippini, N., Smith, S.M., 2009. Group comparison of resting-state FMRI data using multi-subject ICA and dual regression. Neuroimage 47 (Suppl. 1), S148.

Betzel, R.F., Byrge, L., He, Y., Goni, J., Zuo, X.N., Sporns, O., 2014. Changes in structural and functional connectivity among resting-state networks across the human lifespan. Neuroimage 102 (Pt 2), 345–357.

Bijsterbosch, J., Harrison, S., Duff, E., Alfaro-Almagro, F., Woolrich, M., Smith, S., 2017. Investigations into within- and between-subject resting-state amplitude variations. Neuroimage 159, 57–69.

Blazquez, E., Velazquez, E., Hurtado-Carneiro, V., Ruiz-Albusac, J.M., 2014. Insulin in the brain: its pathophysiological implications for States related with central insulin resistance, type 2 diabetes and Alzheimer's disease. Front. Endocrinol. 5, 161.

Brant-Zawadzki, M., Fein, G., Van Dyke, C., Kiernan, R., Davenport, L., de Groot, J., 1985. MR imaging of the aging brain: patchy white-matter lesions and dementia. AJNR Am. J. Neuroradiol. 6, 675–682.

Caballero-Gaudes, C., Reynolds, R.C., 2017. Methods for cleaning the BOLD fMRI signal. Neuroimage 154, 128–149.

Chan, M.Y., Alhazmi, F.H., Park, D.C., Savalia, N.K., Wig, G.S., 2017. Resting-state network topology differentiates task signals across the adult life span. J. Neurosci. 37, 2734–2745.

Chan, M.Y., Park, D.C., Savalia, N.K., Petersen, S.E., Wig, G.S., 2014. Decreased segregation of brain systems across the healthy adult lifespan. Proc. Natl. Acad. Sci. U. S. A. 111, E4997–E5006.

Couvy-Duchesne, B., Blokland, G.A., Hickie, I.B., Thompson, P.M., Martin, N.G., de Zubicaray, G.I., McMahon, K.L., Wright, M.J., 2014. Heritability of head motion during resting state functional MRI in 462 healthy twins. Neuroimage 102 (Pt 2), 424–434.

Craft, S., 2007. Insulin resistance and Alzheimer's disease pathogenesis: potential mechanisms and implications for treatment. Curr. Alzheimer Res. 4, 147–152.

Dennis, E.L., Thompson, P.M., 2014. Functional brain connectivity using fMRI in aging and Alzheimer's disease. Neuropsychol. Rev. 24, 49–62.

Esposito, F., Aragri, A., Pesaresi, I., Cirillo, S., Tedeschi, G., Marciano, E., Goebel, R., Di Salle, F., 2008. Independent component model of the default-mode brain function: combining individual-level and population-level analyses in resting-state fMRI. Magn. Reson. Imaging 26, 905–913.

Ferreira, L.K., Busatto, G.F., 2013. Resting-state functional connectivity in normal brain aging. Neurosci. Biobehav. Rev. 37, 384–400.

Ferreira, L.K., Regina, A.C., Kovacevic, N., Martin Mda, G., Santos, P.P., Carneiro Cde, G., Kerr, D.S., Amaro Jr., E., McIntosh, A.R., Busatto, G.F., 2016. Aging effects on whole-brain functional connectivity in adults free of cognitive and psychiatric disorders. Cerebr. Cortex 26, 3851–3865.

Filippini, N., MacIntosh, B.J., Hough, M.G., Goodwin, G.M., Frisoni, G.B., Smith, S.M., Matthews, P.M., Beckmann, C.F., Mackay, C.E., 2009. Distinct patterns of brain activity in young carriers of the APOE-epsilon4 allele. Proc. Natl. Acad. Sci. U. S. A. 106, 7209–7214.

Fischl, B., Salat, D.H., van der Kouwe, A.J., Makris, N., Segonne, F., Quinn, B.T., Dale, A.M., 2004. Sequence-independent segmentation of magnetic resonance images. Neuroimage 23 (Suppl. 1), S69–S84.

Fox, M.D., Raichle, M.E., 2007. Spontaneous fluctuations in brain activity observed with functional magnetic resonance imaging. Nat. Rev. Neurosci. 8, 700–711.

Friston, K.J., 2011. Functional and effective connectivity: a review. Brain Connect. 1, 13–36.

Geerligs, L., Renken, R.J., Saliasi, E., Maurits, N.M., Lorist, M.M., 2015. A brain-wide study of age-related changes in functional connectivity. Cerebr. Cortex 25, 1987–1999.

Grady, C., Sarraf, S., Saverino, C., Campbell, K., 2016. Age differences in the functional interactions among the default, frontoparietal control, and dorsal attention networks. Neurobiol. Aging 41, 159–172.

Greicius, M.D., Srivastava, G., Reiss, A.L., Menon, V., 2004. Default-mode network activity distinguishes Alzheimer's disease from healthy aging: evidence from functional MRI. Proc. Natl. Acad. Sci. U. S. A. 101, 4637–4642.

Griffanti, L., Douaud, G., Bijsterbosch, J., Evangelisti, S., Alfaro-Almagro, F., Glasser, M.F., Duff, E.P., Fitzgibbon, S., Westphal, R., Carone, D., Beckmann, C.F., Smith, S.M., 2017. Hand classification of fMRI ICA noise components. Neuroimage 154, 188–205.

Griffanti, L., Salimi-Khorshidi, G., Beckmann, C.F., Auerbach, E.J., Douaud, G., Sexton, C.E., Zsoldos, E., Ebmeier, K.P., Filippini, N., Mackay, C.E., Moeller, S., Xu, J., Yacoub, E., Baselli, G., Ugurbil, K., Miller, K.L., Smith, S.M., 2014. ICA-based artefact removal and accelerated fMRI acquisition for improved resting state network imaging. Neuroimage 95, 232–247.

Hafkemeijer, A., van der Grond, J., Rombouts, S.A., 2012. Imaging the default mode network in aging and dementia. Biochim. Biophys. Acta 1822, 431–441.

Ikram, M.A., Brusselle, G.G.O., Murad, S.D., van Duijn, C.M., Franco, O.H., Goedegebure, A., Klaver, C.C.W., Nijsten, T.E.C., Peeters, R.P., Stricker, B.H., Tiemeier, H., Uitterlinden, A.G., Vernooij, M.W., Hofman, A., 2017. The Rotterdam Study: 2018 update on objectives, design and main results. Eur. J. Epidemiol. 32, 807–850.

Ikram, M.A., van der Lugt, A., Niessen, W.J., Koudstaal, P.J., Krestin, G.P., Hofman, A., Bos, D., Vernooij, M.W., 2015. The Rotterdam Scan Study: design update 2016 and main findings. Eur. J. Epidemiol. 30, 1299–1315.

Jack Jr., C.R., Knopman, D.S., Jagust, W.J., Shaw, L.M., Aisen, P.S., Weiner, M.W., Petersen, R.C., Trojanowski, J.Q., 2010. Hypothetical model of dynamic biomarkers of the Alzheimer's pathological cascade. Lancet Neurol. 9, 119–128.

Jenkinson, M., Bannister, P., Brady, M., Smith, S., 2002. Improved optimization for the robust and accurate linear registration and motion correction of brain images. Neuroimage 17, 825–841.

Jenkinson, M., Beckmann, C.F., Behrens, T.E., Woolrich, M.W., Smith, S.M., 2012. Fsl. Neuroimage 62, 782–790.

Jenkinson, M., Smith, S., 2001. A global optimisation method for robust affine registration of brain images. Med. Image Anal. 5, 143–156.

Jockwitz, C., Caspers, S., Lux, S., Eickhoff, S.B., Jutten, K., Lenzen, S., Moebus, S., Pundt, N., Reid, A., Hoffstaedter, F., Jockel, K.H., Erbel, R., Cichon, S., Nothen, M.M., Shah, N.J., Zilles, K., Amunts, K., 2017. Influence of age and cognitive performance on resting-state brain networks of older adults in a population-based cohort. Cortex 89, 28–44.

Keller, J.B., Hedden, T., Thompson, T.W., Anteraper, S.A., Gabrieli, J.D., Whitfield-Gabrieli, S., 2015. Resting-state anticorrelations between medial and lateral prefrontal cortex: association with working memory, aging, and individual differences. Cortex 64, 271–280.

Kiviniemi, V., Starck, T., Remes, J., Long, X., Nikkinen, J., Haapea, M., Veijola, J., Moilanen, I., Isohanni, M., Zang, Y.-F., Tervonen, O., 2009. Functional segmentation of the brain cortex using high model order group PICA. Hum. Brain Mapp. 30, 3865–3886.

Klaassens, B.L., van Gerven, J.M.A., van der Grond, J., de Vos, F., Moller, C., Rombouts, S., 2017. Diminished posterior precuneus connectivity with the default mode network differentiates normal aging from Alzheimer's disease. Front. Aging Neurosci. 9, 97.

Koch, W., Teipel, S., Mueller, S., Buerger, K., Bokde, A.L., Hampel, H., Coates, U., Reiser, M., Meindl, T., 2010. Effects of aging on default mode network activity in resting state fMRI: does the method of analysis matter? Neuroimage 51, 280–287.

Liu, T.T., 2013. Neurovascular factors in resting-state functional MRI. Neuroimage 80, 339–348.

Logothetis, N.K., 2002. The neural basis of the blood-oxygen-level-dependent functional magnetic resonance imaging signal. Philos. Trans. R. Soc. Lond. B Biol. Sci. 357, 1003–1037.

Miller, K.L., Alfaro-Almagro, F., Bangerter, N.K., Thomas, D.L., Yacoub, E., Xu, J., Bartsch, A.J., Jbabdi, S., Sotiropoulos, S.N., Andersson, J.L., Griffanti, L., Douaud, G., Okell, T.W., Weale, P., Dragonu, I., Garratt, S., Hudson, S., Collins, R., Jenkinson, M., Matthews, P.M., Smith, S.M., 2016. Multimodal population brain imaging in the UK Biobank prospective epidemiological study. Nat. Neurosci. 19, 1523–1536.

Mormino, E.C., Smiljic, A., Hayenga, A.O., Onami, S.H., Greicius, M.D., Rabinovici, G.D., Janabi, M., Baker, S.L., Yen, I.V., Madison, C.M., Miller, B.L., Jagust, W.J., 2011. Relationships between beta-amyloid and functional connectivity in different components of the default mode network in aging. Cerebr. Cortex 21, 2399–2407.

Musen, G., Jacobson, A.M., Bolo, N.R., Simonson, D.C., Shenton, M.E., McCartney, R.L., Flores, V.L., Hoogenboom, W.S., 2012. Resting-state brain functional connectivity is altered in type 2 diabetes. Diabetes 61, 2375–2379.

Nashiro, K., Sakaki, M., Braskie, M.N., Mather, M., 2017. Resting-state networks associated with cognitive processing show more age-related decline than those associated with emotional processing. Neurobiol. Aging 54, 152–162.

Ng, K.K., Lo, J.C., Lim, J.K.W., Chee, M.W.L., Zhou, J., 2016. Reduced functional segregation between the default mode network and the executive control network in healthy older adults: a longitudinal study. Neuroimage 133, 321–330.

Peters, R., 2006. Ageing and the brain. Postgrad. Med. J. 82, 84–88.

Power, J.D., Plitt, M., Laumann, T.O., Martin, A., 2017. Sources and implications of whole-brain fMRI signals in humans. Neuroimage 146, 609–625.

Pruim, R.H., Mennes, M., Buitelaar, J.K., Beckmann, C.F., 2015. Evaluation of ICA-AROMA and alternative strategies for motion artifact removal in resting state fMRI. Neuroimage 112, 278–287.

Ritchie, S.J., Cox, S.R., Shen, X., Lombardo, M.V., Reus, L.M., Alloza, C., Harris, M.A., Alderson, H., Hunter, S., Neilson, E., Liewald, D.C.M., Auyeung, B., Whalley, H.C., Lawrie, S.M., Gale, C.R., Bastin, M.E., McIntosh, A.M., Deary, I.J., 2017. Sex Differences in the Adult Human Brain: Evidence from 5,216 UK Biobank Participants bioRxiv (version 2 April 14, 2017).

Sala-Llonch, R., Bartres-Faz, D., Junque, C., 2015. Reorganization of brain networks in aging: a review of functional connectivity studies. Front. Psychol. 6, 663.
Salimi-Khorshidi, G., Douaud, G., Beckmann, C.F., Glasser, M.F., Griffanti, L., Smith, S.M., 2014. Automatic denoising of functional MRI data: combining independent component analysis and hierarchical fusion of classifiers. Neuroimage 90, 449–468.
Sheline, Y.I., Morris, J.C., Snyder, A.Z., Price, J.L., Yan, Z., D'Angelo, G., Liu, C., Dixit, S., Benzinger, T., Fagan, A., Goate, A., Mintun, M.A., 2010a. APOE4 allele disrupts resting state fMRI connectivity in the absence of amyloid plaques or decreased CSF Abeta42. J. Neurosci. 30, 17035–17040.
Sheline, Y.I., Raichle, M.E., Snyder, A.Z., Morris, J.C., Head, D., Wang, S., Mintun, M.A., 2010b. Amyloid plaques disrupt resting state default mode network connectivity in cognitively normal elderly. Biol. Psychiatry 67, 584–587.
Siman-Tov, T., Bosak, N., Sprecher, E., Paz, R., Eran, A., Aharon-Peretz, J., Kahn, I., 2016. Early age-related functional connectivity decline in high-order cognitive networks. Front. Aging Neurosci. 8, 330.
Smith, S.M., Vidaurre, D., Beckmann, C.F., Glasser, M.F., Jenkinson, M., Miller, K.L., Nichols, T.E., Robinson, E.C., Salimi-Khorshidi, G., Woolrich, M.W., Barch, D.M., Ugurbil, K., Van Essen, D.C., 2013. Functional connectomics from resting-state fMRI. Trends Cognit. Sci. 17, 666–682.
Song, J., Birn, R.M., Boly, M., Meier, T.B., Nair, V.A., Meyerand, M.E., Prabhakaran, V., 2014. Age-related reorganizational changes in modularity and functional connectivity of human brain networks. Brain Connect. 4, 662–676.
Sperling, R., 2011. Potential of functional MRI as a biomarker in early Alzheimer's disease. Neurobiol. Aging 32 (Suppl. 1), S37–S43.
Sun, J., Tong, S., Yang, G.Y., 2012. Reorganization of brain networks in aging and age-related diseases. Aging Dis. 3, 181–193.
Tomasi, D., Volkow, N.D., 2012. Aging and functional brain networks. Mol. Psychiatr. 17 (471), 549–558.
Tsvetanov, K.A., Henson, R.N., Tyler, L.K., Davis, S.W., Shafto, M.A., Taylor, J.R., Williams, N., Cam, C., Rowe, J.B., 2015. The effect of ageing on fMRI: correction for the confounding effects of vascular reactivity evaluated by joint fMRI and MEG in 335 adults. Hum. Brain Mapp. 36, 2248–2269.
Tsvetanov, K.A., Henson, R.N., Tyler, L.K., Razi, A., Geerligs, L., Ham, T.E., Rowe, J.B., Cambridge Centre for, A., Neuroscience, 2016. Extrinsic and intrinsic brain network connectivity maintains cognition across the lifespan despite accelerated decay of regional brain activation. J. Neurosci. 36, 3115–3126.
Tzourio-Mazoyer, N., Landeau, B., Papathanassiou, D., Crivello, F., Etard, O., Delcroix, N., Mazoyer, B., Joliot, M., 2002. Automated anatomical labeling of activations in SPM using a macroscopic anatomical parcellation of the MNI MRI single-subject brain. Neuroimage 15, 273–289.
Van Dijk, K.R., Sabuncu, M.R., Buckner, R.L., 2012. The influence of head motion on intrinsic functional connectivity MRI. Neuroimage 59, 431–438.
Wang, K., Liang, M., Wang, L., Tian, L., Zhang, X., Li, K., Jiang, T., 2007. Altered functional connectivity in early Alzheimer's disease: a resting-state fMRI study. Hum. Brain Mapp. 28, 967–978.
Wang, L., Li, Y., Metzak, P., He, Y., Woodward, T.S., 2010. Age-related changes in topological patterns of large-scale brain functional networks during memory encoding and recognition. Neuroimage 50, 862–872.
Wardlaw, J.M., Brindle, W., Casado, A.M., Shuler, K., Henderson, M., Thomas, B., Macfarlane, J., Munoz Maniega, S., Lymer, K., Morris, Z., Pernet, C., Nailon, W., Ahearn, T., Mumuni, A.N., Mugruza, C., McLean, J., Chakirova, G., Tao, Y.T., Simpson, J., Stanfield, A.C., Johnston, H., Parikh, J., Royle, N.A., De Wilde, J., Bastin, M.E., Weir, N., Farrall, A., Valdes Hernandez, M.C., Group, S.C., 2012. A systematic review of the utility of 1.5 versus 3 Tesla magnetic resonance brain imaging in clinical practice and research. Eur. Radiol. 22, 2295–2303.
Winkler, A.M., Ridgway, G.R., Webster, M.A., Smith, S.M., Nichols, T.E., 2014. Permutation inference for the general linear model. Neuroimage 92, 381–397.
Wu, T., Zang, Y., Wang, L., Long, X., Hallett, M., Chen, Y., Li, K., Chan, P., 2007. Aging influence on functional connectivity of the motor network in the resting state. Neurosci. Lett. 422, 164–168.
Yeo, B.T., Krienen, F.M., Sepulcre, J., Sabuncu, M.R., Lashkari, D., Hollinshead, M., Roffman, J.L., Smoller, J.W., Zollei, L., Polimeni, J.R., Fischl, B., Liu, H., Buckner, R.L., 2011. The organization of the human cerebral cortex estimated by intrinsic functional connectivity. J. Neurophysiol. 106, 1125–1165.